Core-Shell ZrO_2/PMMA Composites via Dispersion Polymerization in Supercritical Fluid: Synthesis, Characterization and Mechanism

Yuvaraj Haldorai, Tongqiang Zong, Jae-Jin Shim

School of Chemical Engineering, Yeungnam University, Gyeongsan, Gyeongbuk 712-749, Republic of Korea

Received 1 March 2011; accepted 12 April 2011
DOI 10.1002/app.34688
Published online 11 August 2011 in Wiley Online Library (wileyonlinelibrary.com).

ABSTRACT: Zirconia (ZrO_2) particles of average size 200 nm were synthesized by sol–gel method and formation of composites with poly(methyl methacrylate) (PMMA) via *in situ* radical dispersion polymerization in supercritical carbon dioxide ($scCO_2$) using a commercially available stabilizer poly(dimethylsiloxane)-*g*-pyrrolidone carboxylic acid (Monosil PCA). ZrO_2 particles were first surface-modified by the silane coupling agent methacryloxypropyltrimethoxysilane (MPTMS), which is capable of copolymerizing with methyl methacrylate (MMA) and provide a reactive C=C bond. SEM results revealed uniform morphological characteristics of the composite materials and good dispersions of the ZrO_2 particles. TEM analysis confirmed the core–shell morphology. The incorporation of ZrO_2 particles in the composites was endorsed by FT-IR. The composites were also confirmed by TGA and XRD. The hybrid composites possess interesting thermal and optical transparency characteristics because of the uniform incorporation of ZrO_2 particles in the polymer matrix. In principle, this simple and environmentally friendly synthetic procedure can be employed to prepare other inorganic oxide containing polymer composites. © 2011 Wiley Periodicals, Inc. J Appl Polym Sci 123: 1176–1183, 2012

Key words: composite; dispersion polymerization; supercritical CO_2; surface modification; zirconia particles

INTRODUCTION

Recent years, there has been increasing interest on the elaboration of nanocomposite systems by embedding of inorganic particles into polymeric matrices.[1–3] The introduction of inorganic nanoparticles into a polymer matrix has proved to be an effective method to improve the performance of polymer materials.[4,5] Several methods have been used to produce polymer nanocomposites, such as sol−gel reaction,[6] polymerization via melt-processing[7] and intercalative polymerization[8] depending on the nature of nanoparticles and on the synthetic process of the polymeric matrices. Conventionally, polymerization of monomers and formation of inorganic nanoparticles are separately performed, and the polymer and nanoparticles are mechanically mixed to form nanocomposites.[9] However, it is extremely difficult to disperse the nanoparticles homogeneously into the polymer matrix because of the easy agglomeration of nanoparticles and the high viscosity of the polymer. In recent years, much attention has been paid to the *in situ* synthesis of nanocomposites, particularly core-shell type particles due to their potential applications.[10] The preparation strategy is carried out via polymerization of monomers in the presence of nanofillers. Prior to the dispersion; the nanofillers must be modified with organic materials to improve their compatibility and dispersion. Particularly emulsion polymerization is a traditional method to produce monodispersed inorganic oxide/polymer core-shell composites. Dispersion polymerization has also been reported to be a viable method to prepare core-shell nanocomposites.[10] However, processing of polymers generally employs large quantity of organic solvents that are noxious and harmful to the environment. Thus, the processing with an environmentally benign supercritical fluid such as carbon dioxide offers an attractive alternative to the conventional processing.

Dispersion polymerization in supercritical carbon dioxide ($scCO_2$) has been extensively studied in recent years.[11,12] Dispersion polymerization is characterized by the fact that the monomer and initiator are soluble, whereas the polymer formed is insoluble in the reaction medium. Supercritical CO_2 technology has been widely applied in material science because of its unique characteristics such as low viscosity, high diffusivity and near zero surface tension.[13] CO_2 has a moderate critical temperature (31.1°C) and critical pressure (7.38 MPa). In addition,

Correspondence to: J.-J. Shim (jjshim@yu.ac.kr).
Contract grant sponsor: Korea Research Foundation, Korean Government; contract grant number: KRF-2009-0074769.

it is nontoxic, nonflammable, and chemically inert. Moreover CO_2 offers high mass transport rates and allows *in situ* removal of unreacted monomers and other impurities. Since supercritical CO_2 has a strong solvent power for dissolving many organic compounds and swelling most organic polymers,[14] it has been successfully utilized in the synthesis of polymer/polymer composites.[15,16] Though few studies have been reported based on the polymer/polymer composites, reports on the synthesis of polymer/inorganic oxide composites in $scCO_2$ are scarce in the literature. Yue et al. synthesized macroporous monoliths consisting of silica nanoparticles embedded in poly (methyl methacrylate) (PMMA) via a one step sol–gel process in $scCO_2$.[17] Recently, PMMA/SiO_2,[18] PS/C_{60},[19] PVAc/SiO_2[20] and PS/SiO_2[21] nanocomposites were also synthesized in $scCO_2$. More recently, we have synthesized PMMA/TiO_2[22] and PHEMA/Fe_3O_4[23] nanocomposites. Particularly there has been no report in the literature based on the synthesis of PMMA/ZrO_2 composites via dispersion polymerization in $scCO_2$. PMMA/ZrO_2 composites have been found to be successful in many applications, for example, organic batteries, microelectronics, nonlinear optics, sensors, and organic field-effect transistor.

In this article, ZrO_2 particles are synthesized by sol–gel method and the formation of composites with PMMA via *in situ* radical dispersion polymerization of MMA in the presence of surface-modified ZrO_2 in $scCO_2$. The resulting composites are characterized by FT-IR, SEM, TEM, XRD, TGA and UV. In addition, the thermal degradation and glass transition temperature of PMMA/ZrO_2 hybrid composites are investigated.

EXPERIMENTAL

Materials

MMA (Aldrich) was purified by passing through a neutral alumina column to remove the inhibitor and then bubbled with nitrogen to remove dissolved oxygen. A commercially available Monosil PCA (Uniquema) was used as a polymeric stabilizer. Zirconium *n*-butoxide, acetic acid, *n*-butyl alcohol, MPTMS and polyethylene glycol (PEG $M_W = 10{,}000$ g mol^{-1}) were obtained from Aldrich and used as received. Ultra high purity CO_2 (99.999%) was purchased from Deokyang Energy Co. The initiator 2,2′-azobisisobutyronitrile (AIBN, Aldrich) was recrystallized with absolute methanol. Toluene (Aldrich) was distilled over CaH_2 prior to use.

Synthesis of zirconia particles by sol–gel method

The zirconia particles were obtained by sol–gel method according to the procedure given in the literature.[24] We slightly modified the procedure. In a typical experiment, a homogeneous hydrolysis solution was prepared by mixing 6×10^{-3} M PEG, 2 M acetic acid water and *n*-butyl alcohol in an ultrasonic bath. To this mixture, 1 M zirconium *n*-butoxide was added. The resulting solution was stirred continuously at 35°C for 24 h. Then, the homogeneous white color sol was heated at 150°C for 6 h to remove the solvents and organic residues. The obtained white powder was dried in a vacuum at 60°C for 24 h. In the hydrolysis and condensation reactions, acetic acid acts as a catalyst to influence the gelation process. The formation reactions are as follows.

$$\text{Hydrolysis}: Zr(OR)_4 + H_2O \rightarrow Zr(OR)_3(OH) + ROH \quad (1)$$

$$\text{Condensation}: Zr(OR)_3(OH) + Zr(OR)_4 \rightarrow (RO)_3Zr\text{-}O\text{-}Zr(OR)_3 + ROH \quad (2)$$

$$Zr(OR)_3(OH) + Zr(OR)_3(OH) \rightarrow (RO)_3Zr\text{-}O\text{-}Zr(OR)_3 + H_2O \quad (3)$$

Grafting of MPTMS onto ZrO_2 particles

The grafting reaction was carried out according to the given procedure.[25] After dispersing 5.0 g of ZrO_2 particles in 100 mL of toluene, 10 g of MPTMS was added and then the solution was stirred under argon atmosphere for 24 h at room temperature. The surface-modified ZrO_2 was isolated by centrifugation and washed three times with toluene. Finally, it was dried under vacuum at 40°C for 24 h.

Synthesis of PMMA/ZrO_2 composite in $scCO_2$

In a typical experiment, 0.1 g of surface-modified ZrO_2 was dispersed into 1.0 g of MMA under sonication to form a suspension, and the suspension was transferred into a 10 mL high pressure reactor. To this, 0.01 g of AIBN and 0.05 g of stabilizer were added. The reactor was sealed and liquid CO_2 was added to approximately one half of the cell volume. The temperature was then gradually increased to 65°C. As the reaction vessel was heated, the remaining CO_2 was added to the system until the desired pressure of 345 bar was reached. The polymerization reaction was allowed to continue with stirring for 12 h. After polymerization, the reactor was cooled in an ice water bath and the unreacted MMA was extracted with liquid CO_2 at the flow rate of 20 mL min^{-1} for 10 min. The dry product was removed from the reactor and weighed.

Characterization

Fourier transmission infrared spectroscopic (FT-IR) characterization was performed using an Excalibur Series FTS 3000 (BioRad) spectrometer. Microscopic

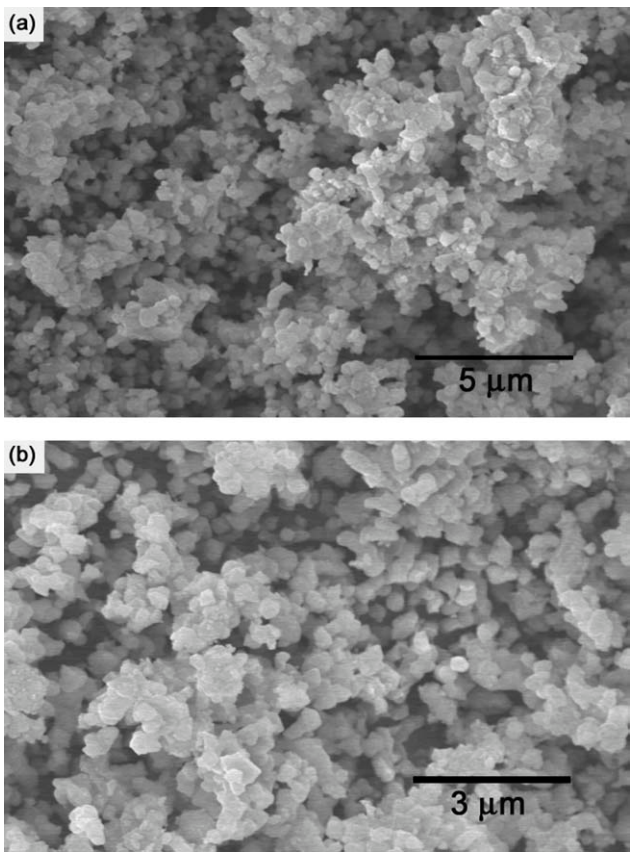

Figure 1 SEM image of as-prepared ZrO_2 (two different magnifications).

images of composite particles were obtained by a Hitachi *S*-4200 field emission scanning electron microscope (FE-SEM). Prior to imaging, the samples were sputter-coated with argon plasma. FE-TEM images were obtained on a field emission transmission electron microscope (Technai G2 F20) operated with an accelerating voltage of 200 kV. Samples for TEM observations were prepared by deposition of the ethanolic dispersions on 200 mesh copper grid. The dispersions were air-dried. XRD patterns were collected on a powder X-ray diffractometer (PANalytical, X'Pert-PRO MPD) with Cu Kα radiation. Thermogravimetric analysis (TGA) and differential thermal analysis (DTG) studies were performed on a TA instruments (SDT Q600 analyzer) from 30 to 600°C at a heating rate of 10°C min^{-1} under nitrogen and air. Differential scanning calorimetry (DSC) was performed on a TA instruments (SDT Q600 analyzer) from 40 to 140°C at a heating rate of 10°C/min under a nitrogen atmosphere. UV- visible transmission spectrum in the 200–800 nm range was obtained using an Agilent 8453 UV-visible spectrophotometer.

RESULTS AND DISCUSSION

To obtain PMMA/ZrO_2 hybrid composite in $scCO_2$, it is necessary to disperse ZrO_2 particles prior to the polymerization. In this work, we used ZrO_2 particles of size 200 nm that were prepared by sol–gel method have well defined quasi-spherical shapes with monodispersity as proved by SEM (Fig. 1). The as-synthesized ZrO_2 particles were not dispersible in CO_2 but were dispersed after modification with MPTMS, which is due to the favorable interaction between MPTMS molecules and CO_2.[17] The procedure involved in the preparation of PMMA/ZrO_2 hybrid composite consisted of two steps. In the first step, silane coupling agent MPTMS was used for the surface-modification of ZrO_2 particles; MPTMS not only converted the ZrO_2 surface into a hydrophobic, but also provided a reactive C=C bond that enabled copolymerization of ZrO_2 with MMA and thereby enhanced interaction between ZrO_2 particles and the polymer. The surface-modified ZrO_2 was characterized by FT-IR (Fig. 2). The spectrum showed characteristic absorption bands: CH_3 (2954–3006 and 1449 cm^{-1}), C=O (1730 cm^{-1}), C=C (1636 cm^{-1}) and Si-O-Zr (1148 cm^{-1}), which indicates the availability of silane group on the surface of ZrO_2 particles.[26] The spectral difference between as-synthesized ZrO_2 and MPTMS-modified ZrO_2 is clearly recognizable. The MPTMS-modified ZrO_2 particles were used as seeds in the dispersion polymerization of MMA stabilized by the polymeric dispersant, monosil PCA in $scCO_2$. It was proven that this method was useful to obtain well-defined composite microparticles. Polymerization reactions were carried out with fixed amount of monomer (10% w/v to CO_2) and stabilizer (10% w/w to monomer), but with varying amount of ZrO_2 particles (2.5, 5, and 10% w/w to monomer). As a comparison, pure PMMA microparticles were also prepared under precisely the same condition. At the

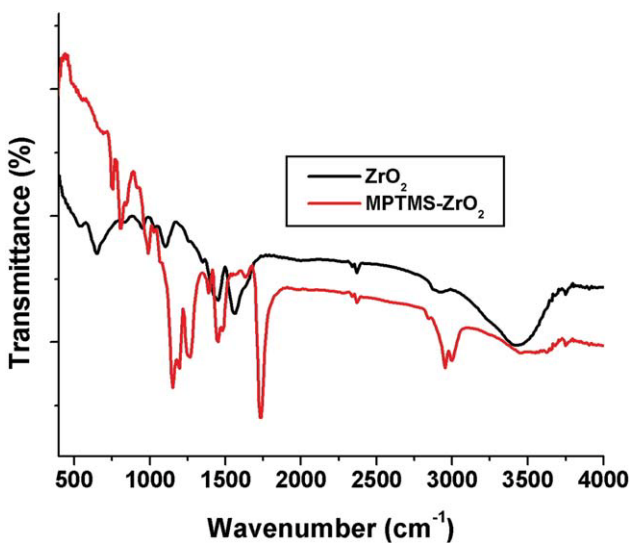

Figure 2 FT-IR spectra of as-prepared ZrO_2 and MPTMS-modified ZrO_2. [Color figure can be viewed in the online issue, which is available at wileyonlinelibrary.com.]

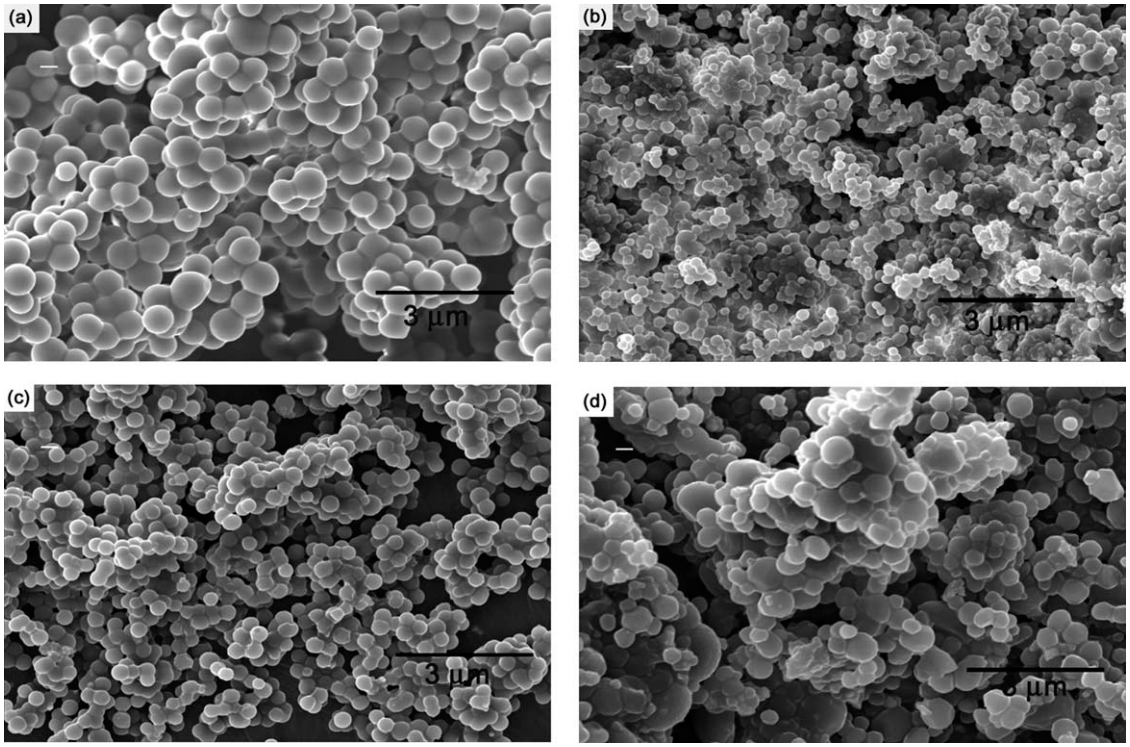

Figure 3 SEM images of (a) pure PMMA, (b) PMMA/ZrO_2-2.5%, (c) PMMA/ZrO_2-5% and (d) PMMA/ZrO_2-10%.

initial stage of polymerization, the ZrO_2 seed particles were well dispersed with stirring as viewed through sapphire window. After 30 min of polymerization the solution became white and it was hard to identify the spin bar inside the reactor. In all the cases, the particles were initially stable, but they appeared to flocculate and coalesce as the reaction proceeds. At higher concentration of ZrO_2, the flocculation increased. A free-flowing white powder remained inside the reaction vessel upon venting the CO_2 after the completion of polymerization. The successful stabilization of polymerizations using monosil PCA resulted in higher yields. Although the size of particles is similar, it can be seen that the conversion of monomer tends to decrease with increasing the amount of ZrO_2. This can be attributed to the fact that, with the increasing amount of ZrO_2 particles in the composites, the percentage of grafting onto the polymer decreases. Figure 3 shows the SEM images of PMMA/ZrO_2 hybrid composites. The composite particles obtained from polymerizations were in the form of spherical particles with relatively narrow particles size distributions for composites with 2.5 and 5% ZrO_2. Slight aggregation between particles were also observed, which is, however, often seen from the dispersion

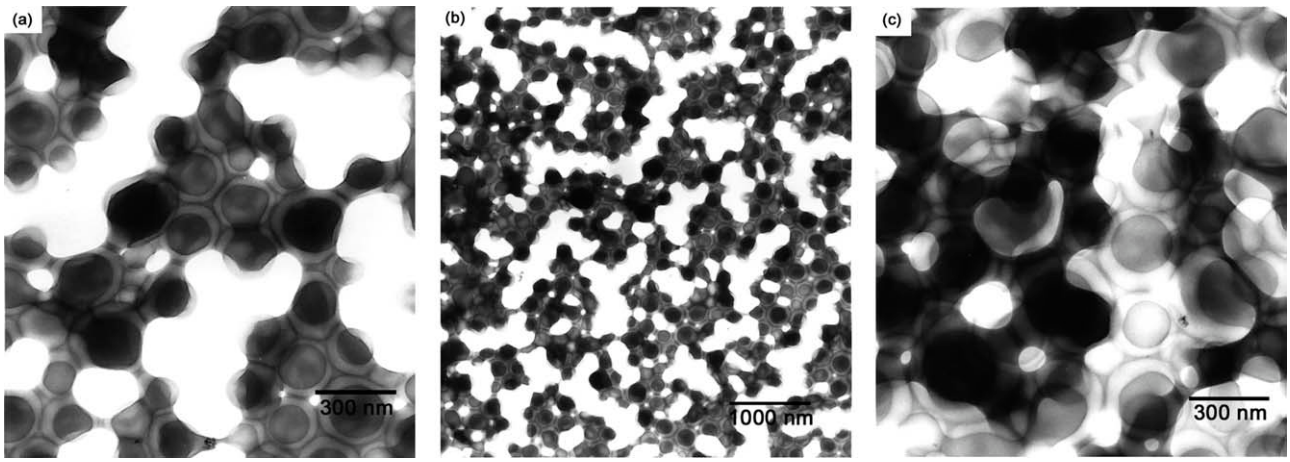

Figure 4 TEM pictures of (a) PMMA/ZrO_2-2.5%, (b) PMMA/ZrO_2-5% and (c) PMMA/ZrO_2-10% composites.

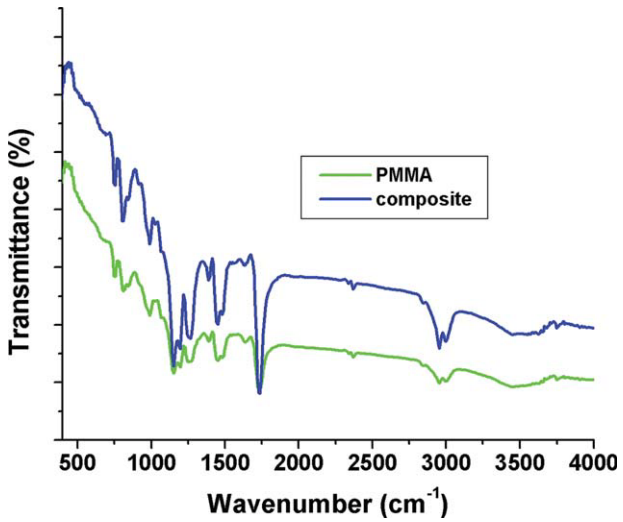

Figure 5 FT-IR spectra of pure PMMA and PMMA/ZrO_2-10% composite. [Color figure can be viewed in the online issue, which is available at wileyonlinelibrary.com.]

polymerization with silicone based stabilizers in $scCO_2$.[27] The results clearly indicate that the monosil PCA stabilizer provided an efficient stabilization for the composite latices to ensure the formation of spherical particles. However, the particles become more agglomerated in the case of composite with 10% ZrO_2. Several big particles were also found, which is evident from the SEM images [Fig. 3(d)]. It is likely that preaggregations of particles were occurred due to the less stabilization of particles in the reaction medium at higher ZrO_2 concentration. This agglomeration is consistent with visual observation of the flocculation during reaction.

To ascertain the composite morphology, TEM analysis was employed. Figure 4 shows the TEM images of PMMA/ZrO_2 hybrid composites, which are clearly evident that the core-shell type morphology was produced successfully with PMMA (light color) as the shell and ZrO_2 as the core (dark). The nature of association between filler and the polymer component showed that almost all ZrO_2 particles were encapsulated by PMMA for composites with 2.5 and 5% ZrO_2 [Fig. 4(a,b)], whereas some ZrO_2 particles exist outside of the polymer surface in the case of composite with 10% ZrO_2. This can be attributed to the fact that, with the increasing amount of ZrO_2 particles in the composite, the percentage of grafting onto the polymer decreases. For composite with 10% ZrO_2, the TEM picture revealed highly agglomerated particles without clear core-shell type image. From the TEM as well SEM micrographs, it is clear that the particle agglomeration is directly proportional to the amount of ZrO_2 loaded. Free PMMA particles that did not contain ZrO_2 were also detected by TEM (data not shown). The presence of these free PMMA particles may be attributed to the fact that the primary particles were incorporated into the composite latices as individual or slightly agglomerated forms via either absorption or copolymerization with MMA, which was stabilized by the polymeric stabilizer, monosil PCA. The amount of free PMMA particles decreases as the ZrO_2 content increases.

Figure 5 shows the FT-IR spectra of PMMA and PMMA/ZrO_2-10% hybrid composite. In the spectrum of PMMA, there are peaks at 2951, 1731, 1449 cm^{-1}, which are assigned to CH, C=O, and CH_3 stretching vibrations respectively. As expected, the spectrum of composite clearly exhibited the absorption bands attributed to both PMMA (2952, 1730, 1448, cm^{-1}) and ZrO_2 (1147 cm^{-1}). The absorption band at 1147 cm^{-1} (Si—O—Zr) indicates that the ZrO_2 particles have been incorporated in the composite.[22,26] Comparing the IR spectrum of composite with MPTMS-modified ZrO_2, the C=C (1632 cm^{-1}) band is not completely disappeared after the polymerization. This may be attributed to fact that the incomplete polymerization of MMA in $scCO_2$.

The possible mechanism for the synthesis of PMMA/ZrO_2 hybrid composite is shown in Scheme 1. First, the MPTMS is chemically bonded on the ZrO_2 surface to introduce vinyl groups (—C=C—). Because of the hydrophobic characteristic of MPTMS, the hydrophilic ZrO_2 becomes amphiphilic after the surface modification by MPTMS. The MPTMS-modified ZrO_2 particles can disperse into the MMA monomer; with adding surfactant, a stable aqueous colloid suspension can be obtained. The surfactant tends to adsorb and orient at fluid–fluid interfaces, with the head group toward the CO_2 phase and the tail group towards the monomer phase. This molecular ordering at the interface reduces the interfacial tension between the two

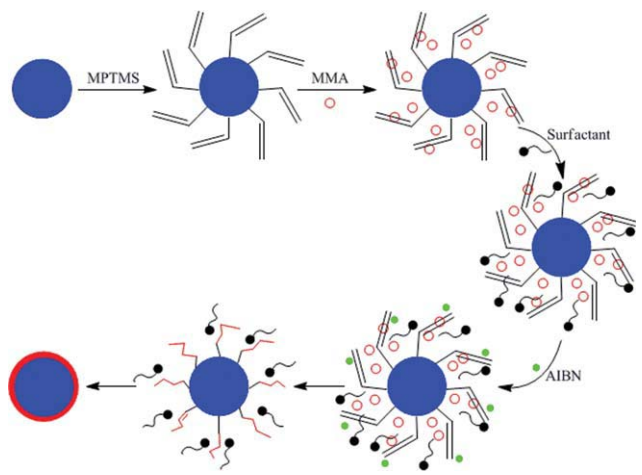

Scheme 1 Schematic representation for the synthesis of PMMA/ZrO_2 composite. [Color figure can be viewed in the online issue, which is available at wileyonlinelibrary.com.]

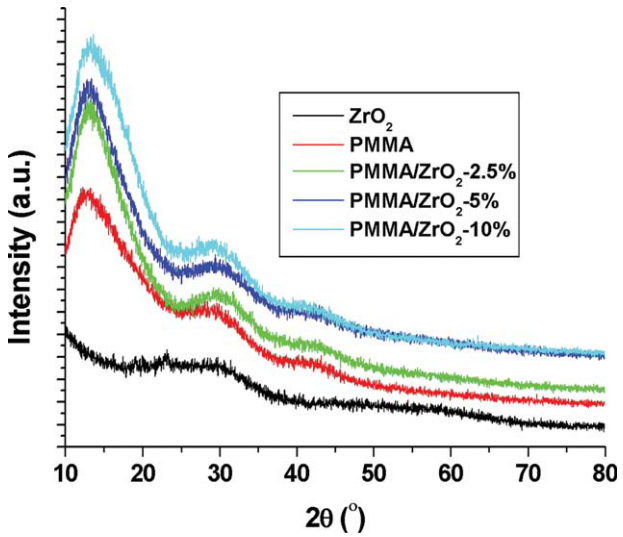

Figure 6 XRD patterns of pure PMMA and PMMA/ZrO_2 composites. [Color figure can be viewed in the online issue, which is available at wileyonlinelibrary.com.]

phases and can thus stabilize the colloids. AIBN is inclined to adsorb towards the hydrophilic domains of ZrO_2 due to its great surface area. At 65°C, AIBN decomposes into primary free radical, and initiates its neighboring vinyl groups of MPTMS that have been bound on the ZrO_2 surface to generate the monomer free radicals. In this case, the monomer radicals are not easily terminated by bimolecular reactions as a result of the low mobility of the solid surface and the low free radical concentration. This monomer free radical can initiate MMA to graft copolymerize and, eventually, PMMA encapsulates on the ZrO_2 surface to obtain core-shell particles. From this process, it can be concluded that, first, the concentration of surfactant is vital for this preparation technique. Too low concentration of surfactant will result in the colloids being unstable, while too high concentration will reduce the grafting efficiency of MMA on the surface of ZrO_2 due to the formation of PMMA latex particles (self-nucleation). Second, the MMA/ZrO_2 ratio should be another important factor to decide the formation of the core-shell particles. Because, there is no micelle existing in the present system, too much hydrophobic MMA will disrupt the stability of the system, resulting in relative low grafting efficiency of MMA onto ZrO_2 surface. Using this technique, other ZrO_2-based polymeric nanohybrids can be fabricated.

XRD patterns of PMMA and PMMA/ZrO_2 hybrid composites are shown in Figure 6. The spectrum of PMMA depicted two broad peaks at $2\theta = 13.3°$ and 29.0°, suggested an amorphous structure of the polymer prepared via dispersion polymerization.[28] The XRD patterns of composites were very similar to that of the PMMA alone, indicating that no additional crystalline order or chain arrangement had been introduced. The results revealed that a thin PMMA layer was formed on the surface of ZrO_2 particles in the process of polymerization. For comparison, the XRD pattern of ZrO_2 particles was also given.

UV-visible transmission spectra of the PMMA/ZrO_2 hybrid composites with different amount of ZrO_2 are depicted in Figure 7. The figure shows that incorporation of ZrO_2 particles causes a slightly declined transparency relative to the pure PMMA. Moreover, the transparency of the composites reduces with increasing ZrO_2 content.[29] However, even for the composite with lowest transparency (PMMA/ZrO_2-10%), it still retains 74% in transmittance relative to the pure PMMA.

Figure 8 illustrates the TGA curves of PMMA and PMMA/ZrO_2 hybrid composites at a heating rate of 10°C min^{-1} under nitrogen and air. All the samples followed a similar decomposition trend, showing a gradual weight loss. The as-prepared PMMA exhibits a three-step weight loss. It is known that radically polymerized PMMA starts to degrade by initiation at the head-to-head linkages (at around 160°C), initiation at the unsaturated ends (at around 270°C), and random initiation along the polymer back bone (at around 350°C).[28] At temperatures above 420°C, the PMMA was completely decomposed. In the case of composites under nitrogen, the thermal decomposition temperature (T_d) for all the steps slightly increased. Whereas, under air the T_d values for the first and second steps increased obviously. However, T_d for the third step increased slightly or even decreased for composite with 10% ZrO_2. Especially for composite with 5% ZrO_2, the second step decreased. This proved that the incorporation of

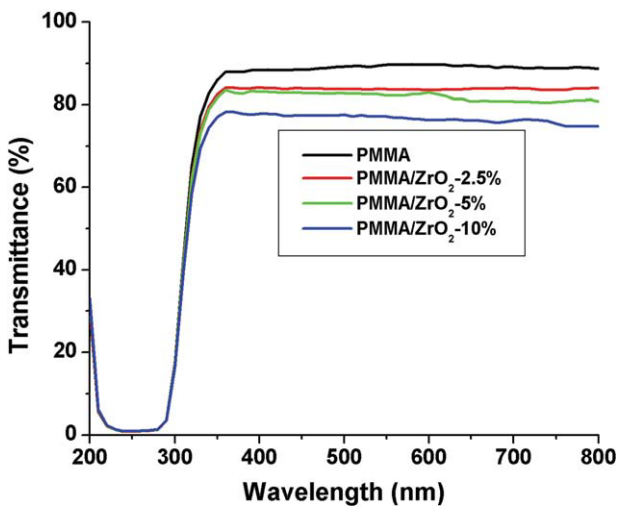

Figure 7 UV-visible transmission spectra of pure PMMA and PMMA/ZrO_2 composites. [Color figure can be viewed in the online issue, which is available at wileyonlinelibrary.com.]

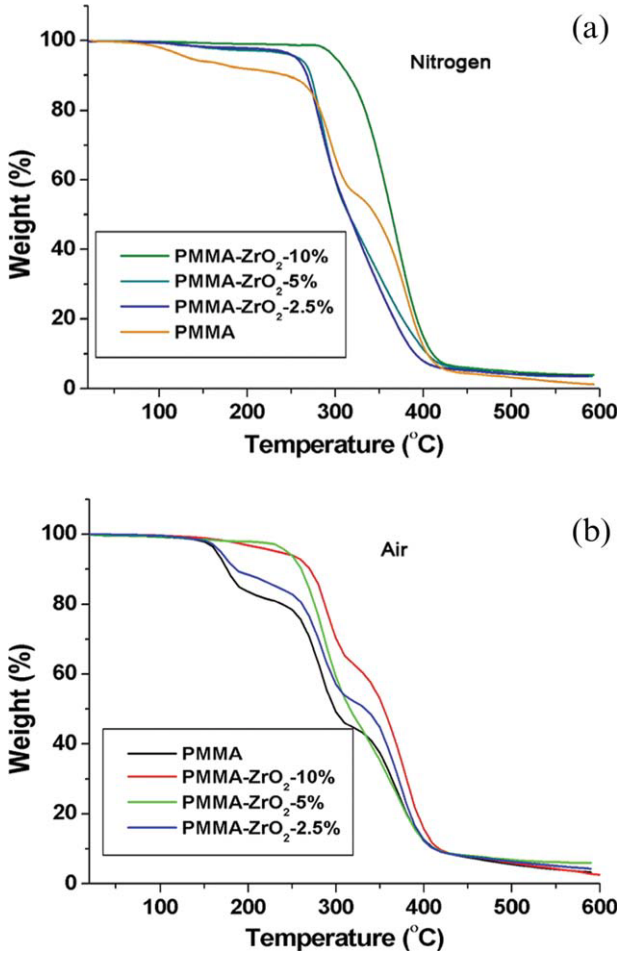

Figure 8 TGA curves of pure PMMA and PMMA/ZrO_2 composites in nitrogen and air. [Color figure can be viewed in the online issue, which is available at wileyonlinelibrary.com.]

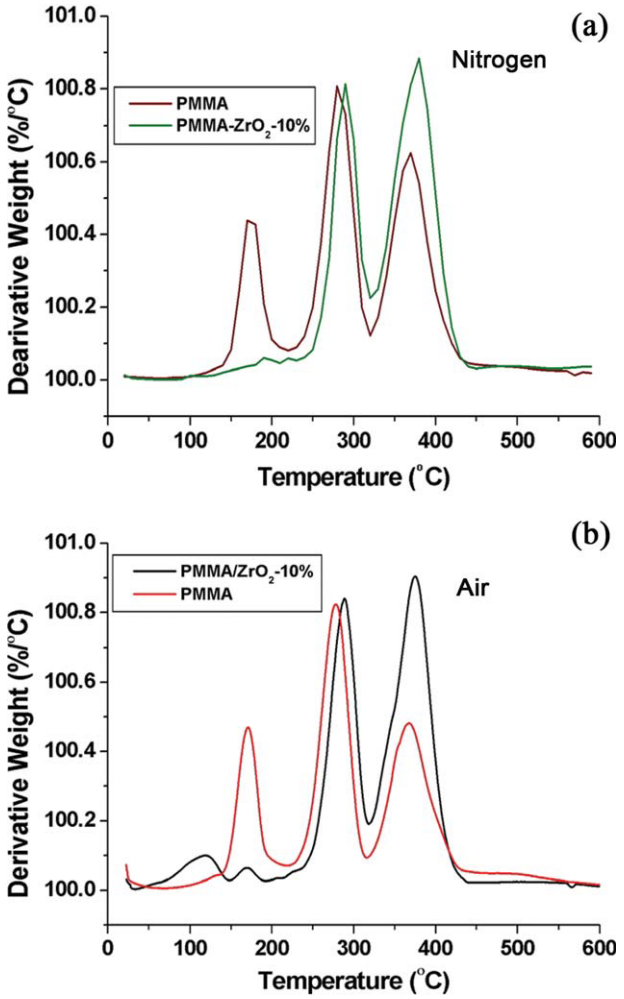

Figure 9 DTG curves of pure PMMA and PMMA/ZrO_2-10% composite in nitrogen and air. [Color figure can be viewed in the online issue, which is available at wileyonlinelibrary.com.]

ZrO_2 particles may have influenced some degradation process of composite, and the mechanisms were different in nitrogen and air.

Figure 9 illustrates the DTG curves of PMMA and PMMA/ZrO_2-10% hybrid composite at a heating rate of 10°C/min under nitrogen and air. Similar like TGA, the thermal degradation of pure PMMA and composite with 10% ZrO_2 under nitrogen and air showed three stages of decomposition. The temperature of maximum reaction rate at a constant heating rate (T_p) obtained from the DTG curves are listed in Table I. As shown in Table I, the T_p values of the three stages in air were lower than those under nitrogen because of oxygen's participation.[30]

The glass-transition behavior of the composites was investigated by DSC. The DSC curves of the four samples are shown in Figure 10. T_g of the pure PMMA and nanocomposites with 2.5, 5 and 10% ZrO_2, determined by DSC were 99.2 and 107.5, 113.04, 118.8°C, respectively. The T_g values increased when the content of the ZrO_2 particles increased. Similar T_g values were observed by others in the literature.[28] It is well known that there are many factors that affect the T_g of a polymer, such as the flexibility of the main chain, the type of substituent, and the configuration. The introduction of the ZrO_2 particles may have restricted the mobility of the

TABLE I
Thermal Degradation (DTG) Values of Pure PMMA and PMMA/ZrO2-10% Composite at a Heating Rate of 10°C/min Under Nitrogen and Air

		T_p (°C)		
Sample	Atmosphere	Stage 1	Stage 2	Stage 3
PMMA	N_2	171.5	279.4	369.8
	air	170.2	278.0	367.9
10% composite	N_2	180.0	289.9	380.1
	air	171.9	288.6	374.9

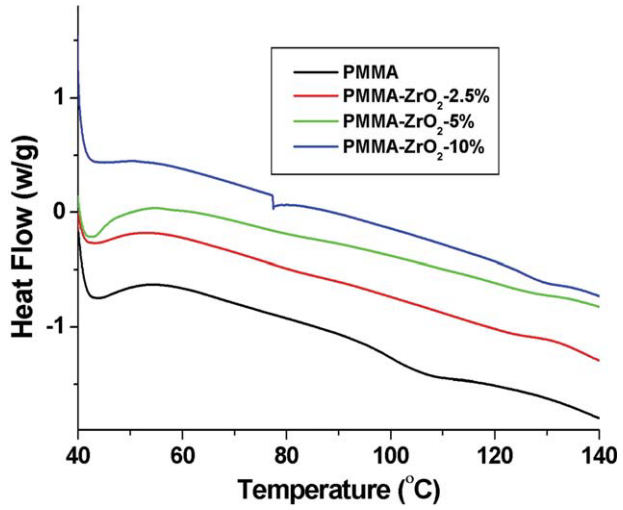

Figure 10 DSC curves of pure PMMA and PMMA/ZrO_2 composites. [Color figure can be viewed in the online issue, which is available at wileyonlinelibrary.com.]

polymer chains, and accordingly, a significant shift in T_g of PMMA toward higher temperatures was observed.

CONCLUSIONS

In summary, we successfully synthesized PMMA/ZrO_2 hybrid composites via *in situ* radical dispersion polymerization in $scCO_2$. TEM images revealed core–shell morphology with an average core size of around 200 nm. FE-SEM analysis demonstrated that the resulting composite particles were spherical in shape with a narrow particle size distribution. TGA analysis carried out both in nitrogen and air showed that the thermal decomposition temperature of each step was affected by the loading of ZrO_2. The introduction of ZrO_2 restricted the mobility of the polymer chains and enhanced the T_g of composites. DTG results showed that the thermal degradation values of the three stages in air were lower than those of nitrogen because of oxygen's participation. UV-visible transmission spectra showed that the PMMA/ZrO_2-10% composite has the lowest transparency and it still retains 74% in transmittance relative to the pure PMMA. This strategy can be easily extended to a vast array of nanoparticles with varied compositions, sizes, and other structural parameters.

This research is done by the project "Human Resources Development for Regional Economy-Leading Industry," supported by the Ministry of Education, Science & Technology (MEST) of Korea and the National Research Foundation of Korea (NRF).

References

1. Mukheerjee, M.; Datta, A.; Chakravorty, D. Appl Phys Lett 1994, 64, 1159.
2. Chen, T. K.; Tien, Y. I.; Wei, K. H. Polymer 2000, 41, 1345.
3. Ramos, J.; Millan, A.; Palacio, F. Polymer 2000, 41, 8461.
4. Okamoto, M.; Morita, S.; Taguchi, H.; Kim, Y. H.; Kotaka, S.; Tateyama, H. Polymer 2000, 41, 3887.
5. Avella, M.; Errico, M. E.; Martuscelli, E. Nano Lett 2001, 4, 213.
6. Noell, J. L. W.; Wilders, G. L.; McGrath, J. E. J Appl Polym Sci 1990, 40, 1177.
7. Vaia, R. A.; Jandt, K. D.; Giannelis, E. P. Macromolecules 1995, 28, 8080.
8. LeBaron, P. C.; Wang, Z. J Appl Clay Sci 1999, 15, 11.
9. Ghosh, K.; Maiti, S. N. J Appl Polym Sci 1996, 60, 323.
10. Zou, H.; Wu, S.; Shen, J. Chem Rev 2008, 108, 3893.
11. Desimone, J. M.; Maury, E. E.; Menceloglu, Y. Z.; McClain, J. B.; Romack, T. J. Science 1994, 265, 356.
12. Canelas, D. A.; Betts, D. E. Macromolecules 1996, 29, 2818.
13. Jessop, P. G.; Leitner, W. Chem Synthesis Using Supercritical Fluids, Weinheim: Wiley-VCH, 1999.
14. Kirby, C. F.; McHugh, M. A. Chem Rev 1999, 99, 565.
15. Watkins, J. J.; McCarthy, T. J. Macromolecules 1994, 27, 4845.
16. Kung, E.; Lesser, A. J.; McCarthy, T. J. Macromolecules 1998, 31, 4160.
17. Yue, B.; Yang, J.; Huang, C. Y.; Dave, R.; Pfeffer, R. Macromol Rapid Commun 2005, 26, 1406.
18. Park, E. J.; Hwang, H. S.; Park, C.; Lim, K. T. Macromol Symp 2007, 249–250, 196.
19. Wang, W.; Howdle, S. M.; Yan, D. Chem Commun 2005, 3939.
20. Charpentier, P. A.; Xu, W. Z.; Li, Z. Green Chem 2007, 9, 768.
21. Do, K. M.; Yuvaraj, H.; Woo, M. H.; Kim, H. G.; Jeong, E. G.; Johnston, K. P.; Lim, K. T. Colloid Polym Sci 2008, 286, 1343.
22. Yuvaraj, H.; Kim, W. S.; Kim, J. T.; Kang, I. P.; Gal, Y. S.; Kim, S. W.; Lim, K. T. Mol Cryst Liq Cryst 2009, 514, 355.
23. Nguyen, V. H.; Haldorai, Y.; Pham, Q. L.; Shim, J. J. J Mater Sci B, 2011, 176, 773.
24. Wang, Y.; Zhang, D.; Shi, L.; Li, L.; Zhang, J. Mater Chem Phys 2008, 110, 463.
25. Tsubokawa, N.; Maruyama, K.; Sone, Y.; Shimomura, M. Polym J 1989, 21, 475.
26. Otsuka, T.; Chujo Y. Polym J 2010, 42, 58.
27. Yates, M. Z.; Li, G.; Shim, J. J.; Maniar, S.; Johnston, K. P.; Lim, K. T.; Webber, S. Macromolecules 1999, 32, 1018.
28. Wang, X.; Wu, L.; Li, J. J Appl Polym Sci 2010, 117, 163.
29. Hu, X.; Zhou, S.; Wu, L. Polymer 2009, 50, 3690.
30. Arisawa, H.; Brill, T. B. Combust Flame 1997, 109, 415.